Neuroradiology (1992) 35: 57–65

Neuro radiology

Investigation of stroke in sickle cell disease by ^{1}H nuclear magnetic resonance spectroscopy

Z. Wang[1], A. R. Bogdan[3], R. A. Zimmerman[1], D. A. Gusnard[1], J. S. Leigh[1], and K. Ohene-Frempong[2]

[1] Department of Radiology and
[2] Division of Hematology, Children's Hospital of Philadelphia, University of Pennsylvania, Philadelphia
[3] Siemens Medical Systems, Aston, Pennsylvania, USA

Received: 2 March 1992

Summary. Localized proton nuclear magnetic resonance spectroscopy (MRS), obtained with stimulated echo and spin echo sequences, MR imaging (MRI) and MR angiography (MRA) were used to study the brain in 13 children and adolescents with sickle cell disease. Regions of interest (ROI) studied by MRS included regions appearing normal on MRI as well as regions showing complications of sickle cell disease, including focal deep white matter areas of high signal intensity (deep white matter ischemia, DWMI) seen on long TR images, focal atrophic brain areas, and infarcts. The findings in these studies are summarized as follows: Normal-appearing regions on MRI have normal MRS. In ROI including small areas of DWMI, lactate elevation was not detected, but the levels of *N*-acetyl-aspartate (NAA) appeared slightly elevated. In areas of DWMI 1–2 cm in size, reduced blood flow could be seen on MRA and lactate elevation could be detected with MRS. When blood flow to a DWMI region was normal, NAA was reduced and there was little lactate elevation, as cell death had already occurred. ROI consisting of atrophic tissue had reduced NAA levels but total creatine levels were not changed. Sometimes lipids, presumably from broken cell membrane, could be detected. In regions of past massive stroke, all metabolites were absent except for small amounts of lactate or lipids.

Key words: Stroke – Cerebrovascular accident – Sickle cell disease – Magnetic resonance imaging – Magnetic resonance angiography – Magnetic resonance spectroscopy

Stroke is one of the most devastating complications of sickle cell disease (SCD) [1]. In children, strokes are usually due to ischemic infarcts and rarely to hemorrhage. The prevalence of stroke in SCD has been reported to be 6–9 % [1]. No age group of sickle cell patients is spared by stroke which, in children, occurs at more than 500 times the rate seen in the general population [1]. Strokes in SCD have a high tendency to recur. In order to prevent recurrence, patients who suffer infarctive stroke are usually placed on chronic transfusion therapy to maintain a high percentage of normal Hb-A-containing red cells. While this regimen is effective in preventing recurrence, it has become an open-ended commitment, as no criteria for its safe discontinuation have been developed. Because of the costs and risks involved in long-term transfusion therapy, it is important to find objective measures which may provide information useful in deciding when transfusion therapy can be safely modified or discontinued. It is also important to develop measures which can detect ischemic changes in the brain prior to the occurrence of stroke so that preventive therapy can be tested and implemented.

Nuclear magnetic resonance (NMR) as a diagnostic tool has the potential ability to provide the relevant information. Magnetic resonance imaging (MRI) has been used to demonstrate major abnormalities in SCD patients following cerebral infarction [2, 3]. Since stroke in SCD is typically due to cerebrovascular disease, information regarding cerebral vasculature and blood flow may have direct clinical relevance. The caliber of cerebral vasculature can be demonstrated by MR angiography (MRA).

In vivo magnetic resonance spectroscopy (MRS), as a method of monitoring the metabolic state of tissue, has been used by many investigators to study stroke [4–15]. The level of lactate, a product of anaerobic metabolism of glucose, can be measured by proton MRS. The level of *N*-acetyl-aspartate (NAA), a metabolite which exists only in neuronal cells, is also measurable [16]. This technique, MRA, and MRI complement each other and together provide information about different but related aspects of the disease state of brain tissue. MRS studies of sickle cell stroke have not been reported previously. We have launched a systematic MR study of stroke in young patients with SCD. In our studies, proton spectra, together with T1- and T2-weighted MRI and MRA have revealed five different patterns.

Methods and materials

All studies were performed on a 1.5 T Siemens Magnatom SP system with A2.1 software utilizing a circularly polarized adult head coil. In one session, MRI, MRA, and MRS examinations were performed. Informed consent was obtained from each patient or from parents.

Table 1. Clinical details of patients

Patient	Sex	Age (years) at time of study	Age (years) at time of stroke(s)	Deficit during strokes	Status at study
n1	F	8	–	–	Normal
n2	F	15	–	–	Normal
n3	M	6	–	–	Normal
n4	M	8	–	–	Normal
s1	F	14.4	1. 13.1 2. 14.1	Headache, blurred vision, L VI and VII palsy headache, VI palsy	Resolved
s2	M	15.1	1. 2.3	L hemiplegia, R monoparesis, aphasia	Triplegial (L > R) /spastic
s3	M	21.1	1. 6.1	Headache, L hemiparesis	L spastic paraplegia
s4	M	22.7	1. 8.0 2. 13.6	L hemiparesis temporal lobe seizures	L spastic hemiplegia
s5	F	22.9	1. 4.0 2. 4.5	L hemiparesis L hemiparesis and seizures	L spastic hemiplegia
s6	F	12.4	1. 10.2 2. 10.8[a]	L arm paresis, headache, aphasia syncope, staring spells	Staring spells
s7	F	16.4	1. 2.0 2. 3.4[a]	L hemiparesis, focal seizure L R hemiparesis	Resolved
s8	M	11.1	1. 3.1 2. 3.2	R hemiparesis, incontinence, aphasia L TIA 1 month prior to CVA	Hemiplegia
s9	M	17.7	1. 3.3 2. 5.0	R hemiplegia, dysphagia R hemiparesis, aphasia, TIAs	Resolved

L, Left; R, right; TIA, transient ischemic attack; CVA, cereberal vascular accident; F, female; M, male
[a] Age at last stroke for patients with multiple recurrent events

The study was approved by the Institutional Review Board of the Children's Hospital of Philadelphia. All patients were in stable condition at the time of the studies. No sedation was used.

We examined 13 patients, 7 male and 6 female, all with Hb SS disease, whose ages ranged from 6 to 23 years, mean 15. The neurologic history of each patient is summarized in Table 1. Nine patients had had one or more clinical strokes. Non-stroke patients are numbered n1–n4 while stroke patients are s1–s9. It has been reported previously that patients without a history of clinical stroke may have visible lesions on MRI [3], while others with such a history may have normal MRI results.

The MRI measurement consisted of standard multislice T1-weighted sagittal spin echo (SE, TR 600 ms, TE 15 ms), and T2-weighted double-echo (TR 3000 ms, TE 30 and 80 ms) axial MR images. The field of view (FOV) was 200 mm. The matrix size was 256×256, and slice thickness 5 mm.

The MRA was obtained with the 3D time-of-flight (3DTOF) method. The 3DTOF pulse sequences were flow compensated FISP sequences [17]. By using short TR and TE, only fresh blood flowing into the region gives high intensity signal since it has not been saturated by radiofrequency (rf) power. The range of parameters was as follows: flip angle 15–25°, TR 30–40 ms, TE 7 ms, FOV 200–230 mm, matrix size 192×256 or 256×256, and 64 partitions with an effective slice thickness of 1.0 mm. After data acquisition, the raw image data were processed with a maximum intensity projection technique. The computer projects a line through the slices along a user-defined viewing angle. The brightest pixel along this line is then placed into the projection image. The procedure is repeated for each pixel in the projection image. Blood flow in cerebral arteries with a diameter larger than 1 mm are visible by MRA. Views from different angles can be obtained, allowing good visualization of normal and abnormal vascular anatomy.

Water suppressed localized proton spectra were obtained with either stimulated spin echo sequence (STEAM) [18] using TR 1.5 s, TE 270 ms and TM 30ms, or spin echo sequence (SE, also called PRESS) [19] with TR 1.5 s, TE 135 or 270 ms. The regions of interest (ROI) were chosen based on T2-weighted MR images (TR 3000 ms, TE 80 ms). The smallest volume used was $2 \times 2 \times 2$ cm^3. We used different pulse sequences for this study because we were in the process of determining which sequence might be preferable for different types of pathology. A comparison between STEAM and SE from a technical viewpoint has been made by Moonen et al. [20]. However, the performance of the pulse sequence may depend on its implementation on the particular spectrometer. The stimulated echo sequence consists of water suppression pulses and three 90° sinc pulses in the presence of magnetic field gradient pulses in three orthogonal directions to achieve spatial localization. Two hundredfold water suppression is usually achieved. The signal comes from the stimulated echo. The SE sequence is similar to STEAM, but two 180° sinc pulses follow the 90° sinc pulse and the signal comes from the second spin echo. For STEAM, only 50% of the total magnetization within ROI contributes to the signal. STEAM is subject to multiquantum effects for the coupled nuclear spin systems such as glutamine, glutamate, and lactate. For SE, 100% of the magnetization can be detected, and the sequence is not subject to the multiquantum effects. For both sequences, small amounts of signal near the vicinity of ROI will leak through. However, due to the use of 180° sinc pulse for refocusing in SE, the leakage is bigger for SE (about 10% of total detected signal for a $3 \times 3 \times 3$ cm^3 volume in a uniform phantom) compared with STEAM (about 5% under the same conditions) in our system. Care was taken in selecting ROI to avoid the contamination of lactate resonance in the ROI by the fat signal from the skull. Usually, 1 cm between the boundary of the ROI and the skull was needed. Processing the MRS data consisted of several steps. First, the eddy current effect was corrected by a second data set taken without water suppression [21]. Then the time domain half spin echo was apodized by a 150 ms width half gaussian to enhance signal to noise ratio. The time domain data were then Fourier transformed into a frequency domain spectrum. The phase of the spectrum was adjusted to yield absorption and dispersion spectra. The baseline of the absorption spectrum was redefined by selecting a number of zero points at different frequencies. Finally, the peak areas of different metabolites in the absorption spectrum were calculated. All data processing was performed with the system software.

Table 2. MR results

Patient	MRI	MRA	MRS
n1	Normal	Normal	Normal
n2	Normal	Normal	Normal
n3	Normal	Normal	Normal
n4	Small DWMI R frontal lobe	Normal	Normal
s1	Normal	Normal	Normal
s2	Old R MCA infarct and L ACA-MCA watershed infarct	R MCA partially visualized, distal L ACA not visualized	Reduced NAA in R infarct
s3	Marked atrophy R hemisphere	R MCA trunk and most distal branches not visualized	Reduced NAA and Cho in atrophic region
s4	Old R MCA infarct; thick skull	R distal ICA, R MCA and some branches of R PCA occluded	Cho, Cr, NAA absent in infarct; small amount of fat/Lac
S5	R MCA R MCA-PCA and L ACA-MCA watershed infarcts	Supraclinoid R ICA occluded, narrow proximal L MCA	No metabolites in infarct; fat elevation R occipital
s6	Old bilateral frontal ACA-MCA watershed infarcts; scattered small DWMI on L posteriorly	Narrow L ICA	Normal
s7	Large bilateral DWMI	R ICA, MCA and ACA occluded, moya-moya collaterals from R PCA	R DWMI Lac elevated; NAA normal
s8	Large L MCA infarct; damaged L occipital pole	L ICA not visualized; cross filling of L ACA from R ICA	L occipital lobe NAA reduced, Lac normal
s9	Old superficial L MCA infarct	L ICA and proximal MCA not visualized; collateral flow from PCA	Normal spectrum near old infarct

L, Left; R, right; DWMI, deep white matter ischemia; ICA, internal corotid artery; MCA, middle cerebral artery; PCA, posterior cerebral artery; ACA, anterior cerebral artery; NAA, *N*-acetyl-aspartate; Cho, choline containing compounds; Cr, creatine; Lac, lactate

Table 3. Metabolite levels in patients with normal MRI and MRA

Patient	Region	Cho	Cr	NAA	Lac	Pulse sequence
s1	Frontal grey	1.8	8.0	8.0	–	SE135
	occipital	1.7	8.0	15.2	–	SE135
n1	Frontal grey	2.3	8.0	9.1	–	SE135
	basal ganglia	1.7	8.0	13.8	–	SE135
n2	Cerebellum	0.9	8.0	6.4	–	STEAM270
	pons	1.0	8.0	9.4	–	STEAM270
n3	Frontal white	2.0	8.0	14.8	–	SE135
	occipital grey	1.3	8.0	10.9	–	SE135

SE135, Spin echo sequence, TE135 ms; STEAM270, STEAM sequence, TE270 ms. Other abbreviations as in Table 2

Major peaks in the proton spectra come from $(CH_3)_3$ group of choline containing compounds at 3.2 ppm, CH_3 group of creatine and creatine phosphate at 3.0 ppm, CH_3 group of NAA at 2.0 ppm and CH_3 group of lactate at 1.3 ppm which appears as a doublet with 7 Hz splitting [22]. The spectroscopy findings are given as the levels of these compounds. The fat signal, when present, appears between 1 and 2 ppm. More recently, it has been demonstrated that the *N*-acetyl methyl resonance at 2 ppm consists of 80–90% of NAA and 10–20% of *N*-acetyl-aspartyl-glutamate [23]. However, our measurement conditions did not allow us to distinguish one from the other.

To obtain the concentration values from measured MRS peak area, one needs to consider the effect of relaxation of the nuclear spins. The T1 and T2 values for the normal adult brain were used to correct the relaxation effects [22]. However, the T1 and T2 values of the metabolites in the pathologic region in stroke patients have not been reported, and the values may vary depending on the tissue state. The concentration of different metabolites varies significantly within a normal brain [22, 24, 25]. The total concentration of creatine and phosphocreatine is relatively uniform throughout the cerebrum in experimental animals and somewhat higher in cerebellum. However, in human cerebrum the total creatine concentration in grey matter is 20% higher than that in white matter [25]. Here the total creatine level was assumed to be 8 mM and uniform. Levels of other metabolites are therefore normalized to creatine. In general, quantifying absolute concentrations remains difficult. The loading of the coil may be different for different patients. The rf excitation and detection sensitivity also vary inside the coil. For STEAM and SE sequences, further complications arise due to interference of the static magnetic field by the eddy currents induced by the magnetic field gradient pulses. For a uniform phantom and constant volume of interest, the signals detected usually change with the location of ROI. However, we may expect to detect the spins in the contralateral control region with the same sensitivity. Therefore, the spectra from contralateral control regions are sometimes taken to serve as an internal reference.

Results

The MRI, MRA, and MRS findings are summarized in Table 2. Based on the MR images, our studies can be divided into five categories: normal MRI regions in stroke and non-stroke patients; small deep white matter foci of ischemia (DWMI) 0.5–1.5 mm in size; DWMI 1–2 cm in size; chronic infarct; and focal atrophy. These divisions are somewhat arbitrary, but form a framework for investigating the spectrum of cerebrovascular disease in patients with SCD. One patient (n4), considered normal clinically, showed small DWMI lesions in MRI, while another (s1), who had a history of neurologic symptoms, had normal MR results. In some patients, more than one category of pathology was present. The MRS results are presented by the MRI categories.

Table 4. Metabolite levels in normal regions of patients with MRI abnormalities

Patient	Region	Cho	Cr	NAA	Lac	Pulse sequence
n4	Basal ganglia	2.0	8.0	10.5	–	SE135
s2	Left cortex	2.0	8.0	13.2	–	STEAM270
s3	Left cortex	1.5	8.0	12.5	–	STEAM270
s4	Left cortex	1.7	8.0	13.4	–	STEAM270
s5	Right cortex white matter	1.5	8.0	18.0	–	STEAM270

Abbreviations is in Tables 2, 3

Table 5. Metabolite levels in regions with small DWMI on MRI

Patient	Region	Cho	Cr	NAA	Lac	Pulse sequence
n4	Frontal white	2.7	8.0	15.2	–	SE135
s6	Internal capsule	2.3	8.0	10.4	–	STEAM270
	Frontal white	1.7	8.0	22.3	–	STEAM270

Table 6. Metabolite levels adjacent to infarcted areas

Patient	Region	Cho	Cr	NAA	Lac	Pulse sequence
s6	Frontal white	2.9	8.0	15.3	–	STEAM270
s9	Frontal white	2.1	8.0	11.3	–	SE135

Table 7. Metabolite levels in regions of large DWMI on MRI

Patient	Region	Cho	Cr	NAA	Lac	Pulse sequence
s7	Frontal white	2.4	8.0	9.9	2.7	SE135
s8	Occipital	1.5	8.0	5.5	–	STEAM270

Normal MRI regions in non-stroke and stroke patients

Three patients (n1, n2, n3) who had no history of clinical stroke had normal MRI. Their MRA studies were also normal. Patient s1 had a history of stroke, but MRI and MRA were normal. Metabolite concentrations obtained from MR spectra collected from different regions of the brains of these 4 patients are given in Table 3, in whom no NAA reduction or lactate elevation was noted.

In 4 patients with MRI abnormalities, we also examined MRS for the normal regions of the brain, as internal concentration standards for the purpose of calibrating the absolute concentration of metabolites in the infarcted regions. We found no abnormality in the spectra from normal regions of patients with various abnormalities elsewhere (Table 4).

Regions containing multiple small DWMI (0.5–1.5 mm) on MRI

These small DWMI foci were widely and sparsely distributed. No significant changes could be found on MRA (Table 5). Since these lesions only accounted for very small fractions of the entire ROI, the MRS signal came mainly from the surrounding tissue. Even if a DWMI region had a high level of lactate, it would not appear in the spectrum above the noise level in the measurement. Therefore, the result should be interpreted as a reflection of the tissue surrounding the small DWMI. We found small DWMI in 1 patient (n4) with no history of stroke (Fig. 1 a). The spectrum from a region containing this small DWMI (Fig. 1 b) is indistinguishable from that of normal brain tissue although the NAA level is on the high side. In patient s6, small DWMI were found in the left frontal lobe white matter and internal capsule. The spectrum in the internal capsule region was normal, but that from the frontal lobe, containing a small DWMI, had significantly elevated NAA (Table 5). MRS from three ROI were obtained; the NAA concentration in the left frontal lobe was verified to be about 20 mM by directly comparing the NAA signal intensity to those in the internal capsule region (Table 5) and from an ROI in the right frontal lobe (Table 6).

Regions containing multiple large DWMI (1–2 cm)

The selected ROI unavoidably contained normal tissue. However, about two thirds of the volume was occupied by the DWMI area itself.

The spectrum obtained with TE 135 ms SE sequence, T2-weighted axial MRI, and the MRA for patient s7 are shown in Fig. 2. The DWMI area could not be distinguished from surrounding normal tissue on T1-weighted MRI. On MRA the right internal carotid, middle cerebral and anterior cerebral arteries were not visualized. With the pulse sequence and the parameters used, the lactate resonance was an antiphase doublet at 1.3 ppm. The metabolite concentrations are shown in Table 7: lactate level was moderately increased, while NAA level was low normal, indicating that the tissue was ischemic, but not permanently damaged.

A second patient (s8, Table 7) had suffered a massive stroke, resulting in tissue loss in most of the left side of the brain (Fig. 3 a). A DWMI on the T2-weighted images, located near the damaged region in the occipital lobe, appeared a little dark on T1-weighted images, indicating tissue loss. MRA (Fig. 3 b) showed normal blood flow to the occipital area. Compared with the values of patient s7, the NAA was decreased and the lactate level was low, but could not be accurately determined; signals appeared at 1–1.5 ppm, corresponding to less than 1 mM lactate signal intensity. A spectrum taken from a region on the left side containing only cerebrospinal fluid (CSF) showed prominent resonance in the same range, presumably from lipids (Fig. 3 d). Since the DWMI was located very close to the region of lost brain tissue and the ROI included some CSF, we believe this signal came from lipids in CSF contained in the ROI, and that lactate was not elevated. The data indicate that the tissue was no longer ischemic, and neuronal loss had already occured.

The values in Table 7 were obtained in the same way as for the normal regions. Clearly, the voxel was not homogeneous, the relaxation times may have been different, and the amount of creatine inside the voxel for patient s8

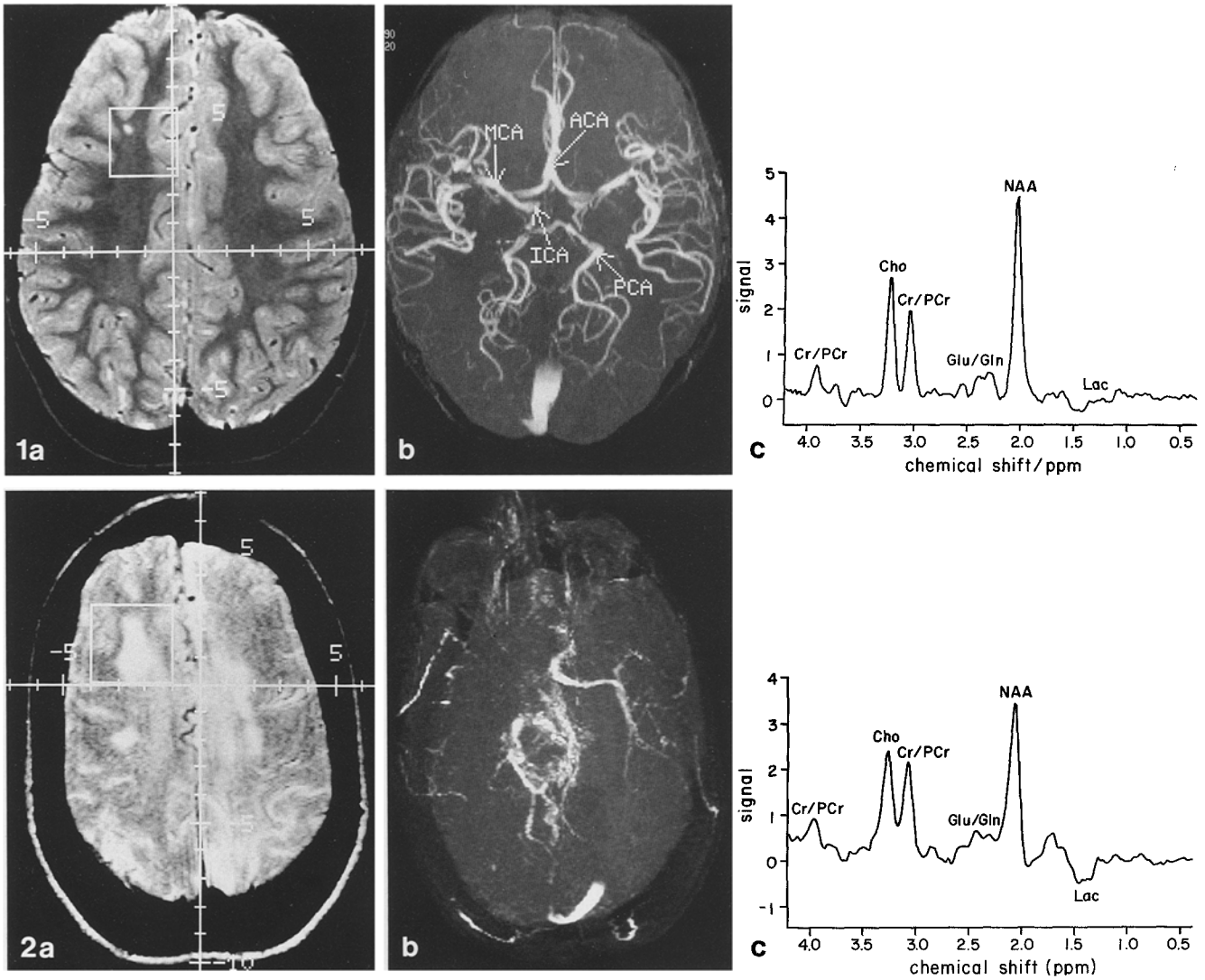

Fig. 1 a–c. Patient n4. **a** T2-weighted axial MRI showing small deep white matter ischemia (DWMI) **b** MRA is normal; *ICA*, internal carotid artery; *MCA*, middle cerebral artery; *PCA*, posterior cerebral artery; *ACA*, anterior cerebral artery. **c** MRS from the region included in the box in **a**. Major peaks in the spectrum are: CH_2 proton of creatine at 3.9 ppm, $(CH_3)_3$ of choline at 3.2 ppm, CH_3 of creatine at 3.0 ppm, and CH_3 of NAA at 2.0 ppm. Glutamine and glutamate can also be seen. Lactate CH_3 would show up at 1.3 ppm as a doublet with 0.1 ppm splitting; the lactate signal is below the noise level

Fig. 2 a–c. Patient s7. **a** T2-weighted axial MRI showing DWMI. **b** MRA shows reduced blood flow to the DWMI region. **c** MRS from the box in **a**. The spectrum was obtained with spin echo sequence, TE 135 ms. Lactate appears at 1.3 ppm as antiphase (negative) signal. *N*-acetyl-aspartate (NAA) level is normal but lactate is elevated

was decreased. However, the values allow us to compare different cases and demonstrate striking differences.

Regions of old massive infarcts

In patient s4, a patient with an old, massive stroke on the right side of the brain, remains of brain tissue in the damaged region were still visible on T1-weighted MRI, although the infarcted region appeared dark. No choline, creatine or NAA was detected by MRS in the old infarct. Some remaining lactate or fat signal could be seen. MRA indicated no flow to the region. In another patient with old massive stroke (s5), no metabolites or lipids were visible by MRS in the infarct. An axial T2-weighted MRI of patient s5 is shown in Fig. 4 a. The spectra of the stroke region and the contralateral normal control region are plotted in Fig. 4 b on the same scale for comparison.

In some cases, the damaged brain was very close to the skull. In order to avoid fat contamination of the spectra, the ROI could not be extended over the entire region. Instead, the ROI included part of the damaged region and some normal brain (Table 6). The spectra had a normal appearance, but a absolute quantification of metabolites was not available. The results were consistent with metabolites no longer being present in the dead tissue; only signals from normal tissues were observed.

Patient s8, discussed above, had a history of massive stroke; brain tissue on the left side of the brain was completely lost and the space was filled with CSF. The CSF

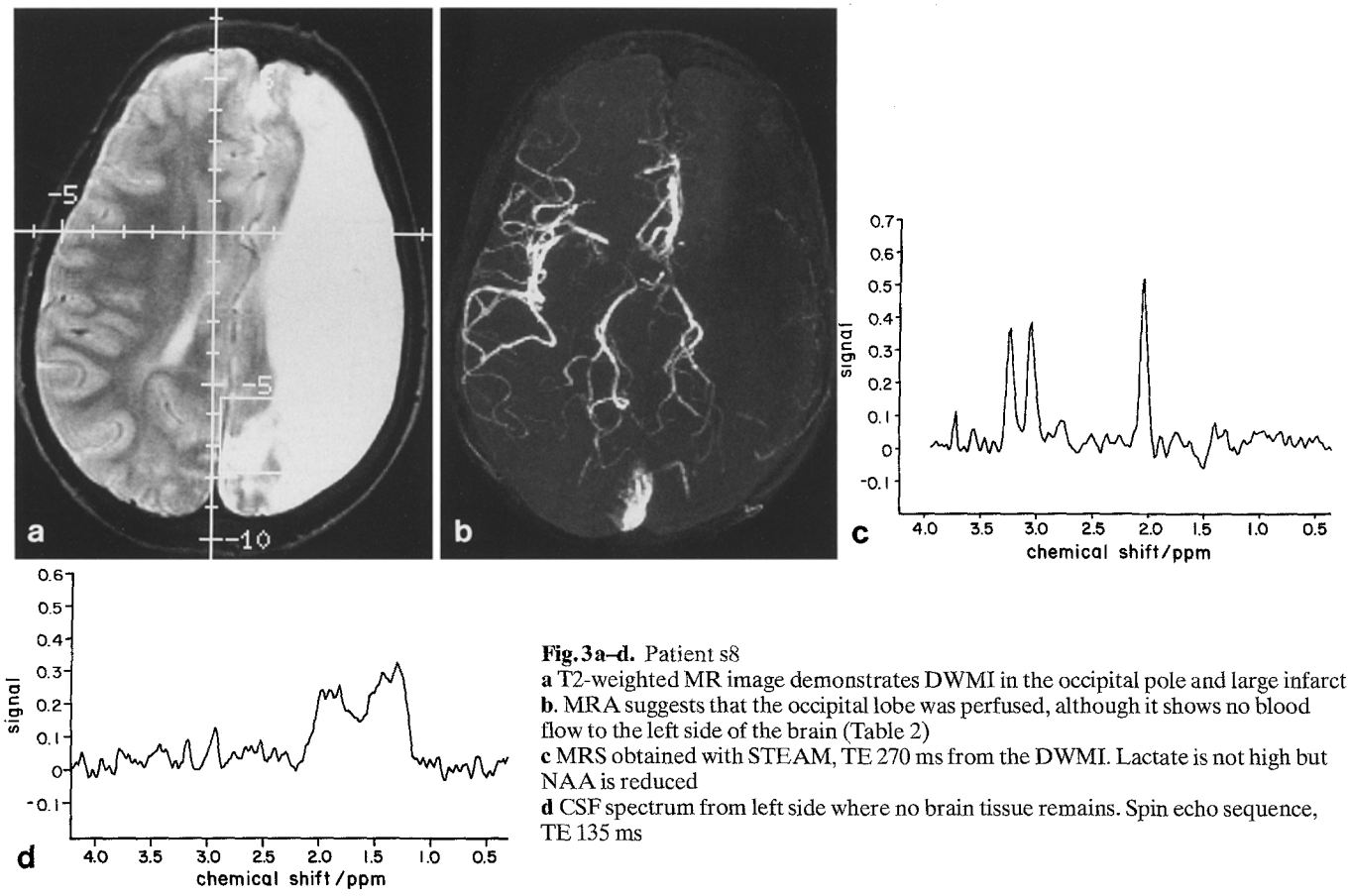

Fig. 3a–d. Patient s8
a T2-weighted MR image demonstrates DWMI in the occipital pole and large infarct
b. MRA suggests that the occipital lobe was perfused, although it shows no blood flow to the left side of the brain (Table 2)
c MRS obtained with STEAM, TE 270 ms from the DWMI. Lactate is not high but NAA is reduced
d CSF spectrum from left side where no brain tissue remains. Spin echo sequence, TE 135 ms

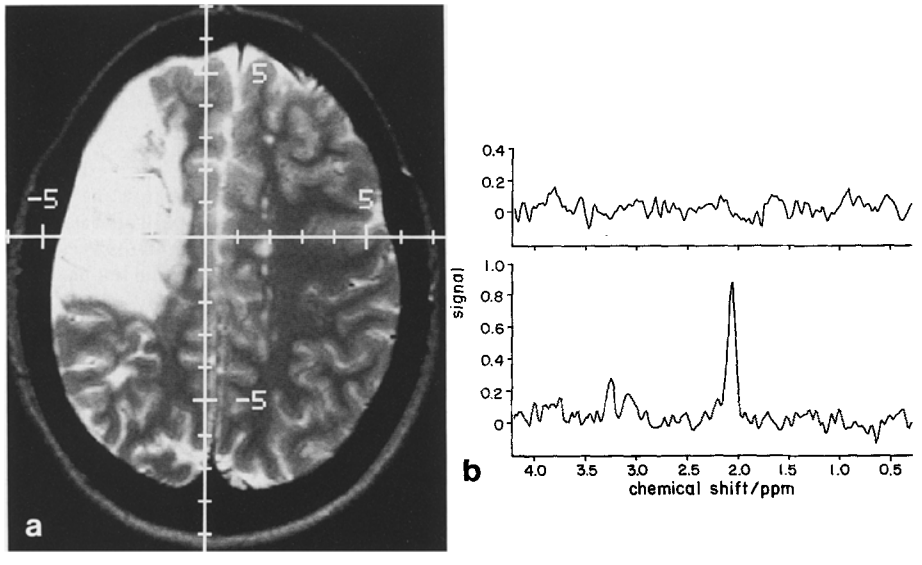

Fig. 4a, b. Patient s5
a MRI shows an old infarct
b MRS. *Upper trace,* large infarct has no remaining metabolites. *Lower trace,* normal contralateral control plotter on the same scale. STEAM sequence, TE 270 ms

spectrum from the region is displayed in Fig. 3d. High-field, high-resolution proton NMR spectroscopy has been used to study human CSF [26, 27]. In normals, only lactate (1.3 ppm) and acetate (1.9 ppm) may give rise to prominent resonance in the 1–2 ppm range; their concentrations are 0.8–2.4 mM and 0.05–4.5 mM respectively [27]. However, the spectrum of patient s8 contained many other resonances, presumably due to lipids and possibly other metabolites.

Regions of focal atrophy

Atrophic tissue can be seen readily on T2-weighted MRI: the CSF space is noticeably increased. The metabolite levels in 2 such patients (s3, s5) are given in Table 8.

In patient s3, the right cortex was markedly atrophic. The blood vessels in the region were severely reduced. The right middle cerebral artery trunk was not visualized on MRA. No lactate elevation was observed. Compared

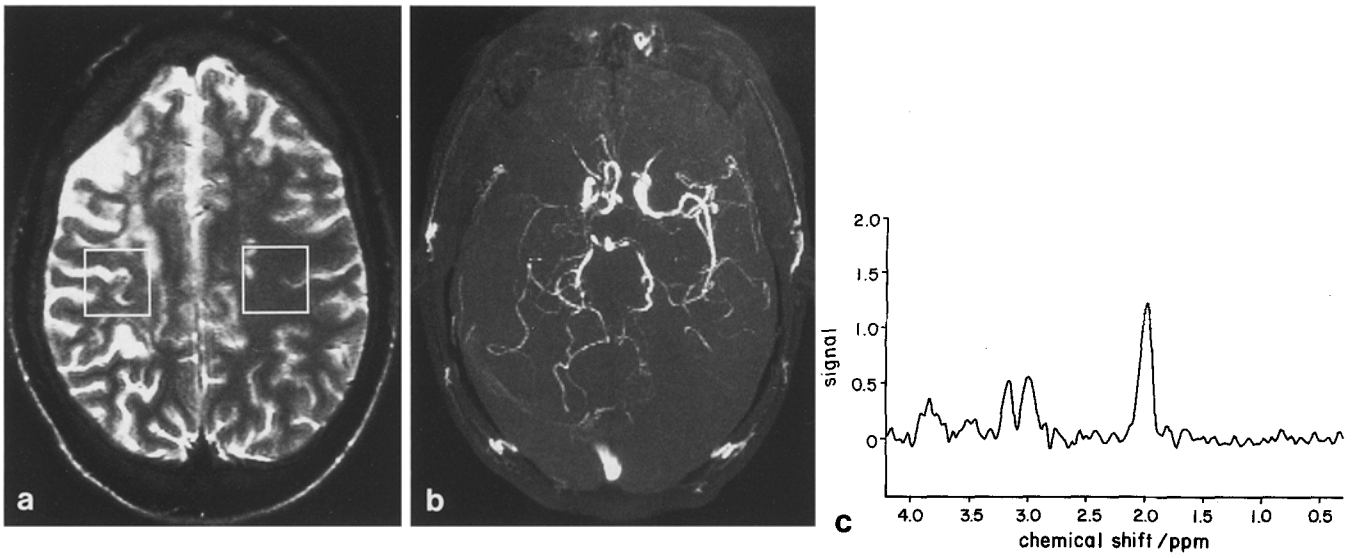

Fig. 5 a–c. Patient s3. **a** T2-weighted image showing atrophy. **b** MRA shows reduced flow in the atrophic region. **c** MRS in pathologic region. Compared with contralateral control MRS region, creatine level remained unchanged, but NAA and choline-containing compounds were reduced

Table 8. Metabolite levels in regions of atrophy

Patient	Region	Cho	Cr	NAA	Lac	Pulse sequence
s3	Right cortex	1.1	8.0	8.6	–	STEAM270
s5	Right cortex	1.5	8.0	10.8	[a]	STEAM270

[a] Fat contamination

with the contralateral control region, NAA was reduced by 25%, indicating neuronal loss choline by 20% and the total creatine level remained unchanged within the range of error of measurement (roughly 10%) (Fig. 4). In patients s5, lipid signal appeared in the spectra from the atrophic region, even though the ROI was far from the skull; it may have come from recently broken cell membranes. The contralateral region was also atrophic and could not therefore serve as a control region for estimation of absolute changes in the metabolites levels.

Discussion

The pathogenesis of cerebrovascular disease in SCD is unclear; initially, it was believed to be caused by occlusion of small vessels by sickled red blood cells. However, angiography has shown that severe large-vessel arterial stenosis and occlusion occur [28, 29]. Strokes in patients with SCD in some regards, have their own characteristics. For example, small DWMI are not a common early finding in other types of stroke. However, our MRS results on sickle cell stroke do have many similarities with the features of conventional stroke.

MRS has been used to study stroke by many investigators [4–16]. The findings depend on the type of stroke, the stage of the pathology and the outcome. In the acute phase, hours to days after the onset, the proton NMR spectra show high levels of lactate, and decreased NAA and creatine signals [6, 7, 9, 10–15]. The lactate level can be as high as 15–20 mM [7], and NAA may decrease to zero [6, 7]; the pH is also low [10]. While some investigators concluded that choline levels do not change in the acute phase of stroke [6], others have observed rather large decreases [7, 11, 13] and attribute this finding to the dilution effect of edema [7]. The diluting effect of edema has been estimated to reduce average metabolite concentration by about a factor of 3 in one case study [7]. In severe cases, lactate was the only metabolite measurable. Eighteen hours to 6 days after the stroke, there is no significant correlation between infarct age and lactate level [14]. The lactate signal may disappear in 14 days [6], but may also persist above the control level for much longer [9, 12]. The recovery of the patient depends on different factors. For example, hyperglycemia causes prolonged deterioration of energy metabolism and acidosis in the ischemic brain [10]. In the worst cases no recovery occurs [11]. Prolonged ischemia may be caused by occlusion or stenosis of a main cerebropetal artery. In addition to regions in which the blood supply is completely cut off, there are so-called penumbra regions, in which metabolism is compromised, and lactate is moderately increased, NAA remains unchanged or slightly decreased, and the pathology may be reversible [8]. In progressive stroke without demarcation of an infarcted zone NAA is decreased but lactate level is not elevated [11]. Prominent fat signals have also been observed soon after acute stroke [6] and in chronic stroke [8, 13], possibly as a result of breakdown of myelin, other phospholipids, and membrane constituents. Months or years after stroke, when patients become stable, the concentrations of the various metabolites are below normal, but NAA reduction is more marked than that of choline or creatine [5, 13].

It has been recognized that the metabolite levels detected by proton MRS depend on age and on location of the ROI, and vary among individuals [30, 31]. The range of variation of metabolite levels in normal individuals has not been determined. About 20% variation in NAA/creatine

ratio may be expected for the same location among people of a given age group. The proton spectra of our patients who had not had a stroke and in the normal-appearing regions of patients who had had a stroke looked normal. The level of NAA did show variations in different regions, part of which reflects the different amount of white and grey matter included in the ROI. The NAA level is 50 % higher in grey matter than in white matter according to high field proton NMR spectroscopy studies on perchloric acid extracts of brain tissue obtained during surgery [25]. However, Table 3 indicates otherwise. It is conceivable that several factors may cause this apparent discrepancy. For example, the nuclear relaxation, properties of NAA in grey and white matter may be different. Higher creatine levels in grey matter also make the NAA levels appear lower, since all concentrations are normalized to 8 mM total creatine. The NAA level of occipital grey matter appears to be higher than that in the frontal region. Moreover, the choline/creatine ratio also varies significantly. Choline is related to myelination of the axons. In the human, myelination goes on until early adulthood and varies depending on the region and the age of the patient.

In acute stroke, it takes 3 h for the lesion to appear on the T2-weighted images, but the change in MR spectra happens minutes after the insult. All our patients had old strokes and were in very stable condition at the time of study. It is therefore not surprising that we found no abnormality in the MR spectra in the regions which looked normal on MRI. Moreover, high lactate level was not detected in any patient in this study.

We did not detect lactate elevation in small DWMI areas, but NAA levels appeared increased. Smaller ROI and more signal averaging are desirable to observe MRS abnormalities such as lactate elevation in the small DWMI. In patients with SCD who have strokes, although they are stable, the pathology appears to be progressive. In the DWMI regions, the spectra have different appearances depending on the disease state. Reduction of NAA follows loss of neurons, while elevation of lactate follows ischemia. The ischemia is no longer present when neuronal damage and tissue loss have resulted. The MRS in the DWMI area of patients s7 is similar to the penumbra phenomena found in stroke patients with compromised metabolism. Permanent damage may not have resulted. In contrast, irreversible damage had already occurred in patient s8.

In the chronically infarcted tissue resulting from old massive stroke, no metabolites are present except small amounts of lipids, so that the spectra from ROI including both dead and normal tissue would have a normal profile except for small amounts of fat.

In atrophic brain, the reduction of NAA and choline is consistent with the expected neuronal loss, while creatine level remains unchanged. Our results may be compared with findings in progressive stroke in which NAA was decreased but no lactate elevation was found [11].

The MRS technique employed here measures the total amount of metabolites in the ROI. In many cases the distribution of lactate and other metabolites within the ROI may not be uniform. In all the cases we examined, the lactate level was always well below the maximum level observed in an acute stroke or in head injury. The DWMI may consist of a badly damaged core and less damaged periphery. The lactate we detected may be highly concentrated in certain locations. Chemical shift imaging with adequate spatial resolution or other advanced spectroscopy techniques are desirable to explore and understand the pathology in finer detail.

Acknowledgements. This study is supported in part by NIH Comprehensive Sickle Cell Center grant P60-HL38632, research funding from Siemens Medical Systems, and NIH grant RR02305. We thank Renee Cecil, Wendi Bulgarelli and Marie Martin for their assistance in patient recruitment and scheduling for MR studies.

References

1. Ohene-Frempong K (1991) Stroke in sickle cell disease: demographic, clinical, and therapeutic considerations. Semin Hematol 28: 213–219
2. Zimmerman RA, Gill F, Goldberg HI, Bilaniuk LT, Hackney DB, Johnson M, Grossman RI, Hecht-Leavitt C (1987) MRI of sickle cell cerebral infarction. Neuroradiology 29: 232–237
3. Pavlakis SG, Bello J, Prohovnik I, Sutton M, Ince C, Mohr JP, Piomelli S, Hilal S, De Vivo DC (1988) Brain infarction in sickle cell anemia: magnetic resonance imaging correlates, Ann Neurol 23: 125–130
4. Bottomley PA, Drayer BP, Smith LS (1986) Chronic adult cerebral infarction studied by phosphorus NMR spectroscopy. Radiology 160: 763–766
5. Hubesch B, Marinier DS, Hetherington HP, Twieg DB, Weiner MW (1989) Clinical MRS studies of the brain. Invest Radiol 24: 1039–1042
6. Fenstermacher MJ, Narayana PA (1990) Serial proton magnetic resonance spectroscopy of ischemic brain injury in humans. Invest Radiol 25: 1034–1039
7. Bruhn H, Frahm J, Gyngell ML, Merboldt KD, Hanicke W, Sauter R (1989) Cerebral metabolism in man after acute stroke: new observations using localized proton NMR spectroscopy. Magn Reson Med 9: 126–131
8. Berkelbachvan der Sprenkel JW, Luyten PR, Rijen PC van, Tulleken CA, Hollander JA den (1988) Cerebral lactate detected by regional proton resonance spectroscopy in a patient with cerebral infarction. Stroke 19: 1556–1560
9. Graham GD, Howseman AM, Rothman DL, et al. (1991) Proton magnetic resonance spectroscopy of metabolites after cerebral infarction in humans. Stroke 22: 143
10. Levine SR, Welch KM, Helpern JA, Chopp M, Bruce R, Selwa J, Smith MB (1988) Prolonged deterioration of ischemic brain energy metabolism and acidosis associated with hyperglycemia; human cerebral infarction studied by ^{31}P NMR spectroscopy. Ann Neurol 23: 416–418
11. Ott D, Ernst T, Hennig J (1990) In vivo ^{1}H spectroscopy in cerebral ischemia. Society of Magnetic Resonance in Medicine, 9th Annual Meeting, New York, p 1011
12. Rijen PC van, Luyten PR, Hollander JA den, Tulleken CAF (1989) Prolonged elevation of cerebral lactate detected with ^{1}H NMR spectroscopy in patients with focal cerebral ischemia. Society of Magnetic Resonance in Medicine, 8th Annual Meeting, Amsterdam, p 374
13. Duyn JH, Hugg JW, Matson GB, Maudsley AA, Weiner MW (1991) ^{1}H and ^{31}P spectroscopic imaging of human brain infarction. Society of Magnetic Resonance in Medicine, 10th Annual Meeting, San Francisco, p 225
14. Mathews VP, Barker PB, Blackband SJ, Chatham JC, Bryan RN (1991) ^{1}H NMR spectroscopy of acute cerebral infarction. Society of Magnetic Resonance in Medicine, 10th Annual Meeting, San Francisco, p 226

15. Petroff OAC, Graham GD, Blamire AM, Al-Rayess M, Kim J, Fayad F, Brass LM, Rothman DL, Shulman RG, Prichard JW (1991) ^{1}H spectroscopic imaging of strokes in man: histopathology correlates of spectral changes. Society of Magnetic Resonance in Medicine, 10th Annual Meeting, San Francisco, p 227
16. Birken DL, Odendorf WH (1989) N-acetyl-L-aspartic acid: a literature review of a compound prominent in ^{1}H NMR spectroscopic studies of brain. Neurosci Biobehav Rev 13: 23–31
17. Edelman RR, Mattle HP, Atkinson DJ, Hoogewoud HM (1990) MR angiography. AJR 154: 937–946
18. Frahm J, Bruhn H, Gyngell ML, Merboldt KD, Haenicke W, Sauter R (1989) Localized high resolution proton NMR spectroscopy using stimulated echoes: initial applications to human brain in vivo. Magn Reson Med 9: 79–93
19. Ordidge RJ, Bendall MR, Gorden RE, Connelly A (1985) Volume selection for in vivo biological spectroscopy. In: Govil G, Khetrapal CL, Saran A (eds) Magnetic resonance in biology and medicine. Tata McGraw Hill, New Delhi, p 387
20. Moonen CTW, Kienlin M von, Zijl PCM van, Cohen J, Gillen J, Daly P, Wolf G (1989) Comparison of single-shot localization methods (STEAM and PRESS) for in vivo proton NMR spectroscopy. NMR Biomed 2: 201–208
21. Klose U (1990) In vivo proton spectroscopy in presence of eddy currents. Magn Reson Med 14: 26–30
22. Frahm J, Bruhn H, Gyngell ML, Merboldt KD, Haenicke W, Sauter R (1989) Localized proton NMR spectroscopy in different regions of the human brain in vivo. Magn Reson Med 11: 47–63
23. Frahm J, Michaelis T, Merboldt K-D, Hanicke W, Gyngell ML, Bruhn H (1991) On the N-acetyl methyl resonance in localized 1H NMR spectra of human brain in vivo. NMR Biomed 4: 201–204
24. Frahm J, Bruhn H, Michaelis KD, Merboldt KD, Gyngell ML, Hanicke W (1990) Regional differences of metabolites in human brain in vivo as detected by proton NMR spectroscopy using 1–8 ml volume of interest. Societa of Magnetic Resonance in Medicine, 9th Annual Meeting, New York, p 1006
25. Petroff OA, Spencer DD, Alger JR, Pritchard JW (1989) High field proton magnetic resonance spectroscopy of human cerebrum obtained during surgery for epilepsy. Neurology 39: 1197–2202
26. Petroff OAC, Yu RK, Ogino T (1986) High-resolution proton magnetic resonance analysis of human cerebrospinal fluid. J Neurochem 47: 1270
27. Commodari F, Arnold DL, Sabctury BC, Shoubrige EA (1991) ^{1}H NMR characterization of normal human cerebrospinal fluid and the detection of methylmalonic acid in a vitamin B12 deficient patient. NMR Biomed 4: 192–200
28. Stockman JA, Nigro MA, Miskin MM, Oski FA (1972) Occlusion of large cerebral vessels in sickle cell anemia. N Engl J Med 287: 846
29. Merkel KHH, Ginsberg PL, Parker JC, Post MJD (1978) Cerebrovascular disease in sickle cell anemia: a clinical pathological correlation. Stroke 9: 45
30. Knaap MS van der, Grond J van der, Rijen PR van, Luyten PR, Valk J (1989) Age-dependent changes in localized proton and phosphorus spectra of the brain in healthy children from birth till sixteen years. Society of Magnetic Resonance in Medicine, 8th Annual Meeting, Amsterdam, p 376
31. Huppi P, Posse S, Lazeyras F, Bossi E, Herschkowitz N (1991) Age-dependent changes in 1H-MR spectroscopy in human brain. American Society for Neurochemistry 22nd. Annual Meeting, Charleston, South Carolina, p 206

Z. Wang, Ph. D.
MRI Unit
Department of Radiology
Children's Hospital of Philadelphia
34th Street and Civic Blvd.
Philadelphia, PA 19104, USA